Vol. 22, n.°4, pp. 181-190, 2023
Revista UIS Ingenierías
Página de la revista: https://revistas.uis.edu.co/index.php/revistauisingenierias

Corrosion resistance of nitrogenated high-carbon martensitic stainless steel designed and produced at nitrogen low pressures

Resistencia a la corrosión de un acero inoxidable martensítico nitrogenado con alto contenido de carbono diseñado y producido a bajas presiones de nitrógeno

Pablo Miguel Coha-Vesga [1a], Guilherme Yuuki-Koga [2a], Martin Emilio Mendoza-Oliveros [1b], Francisco Gil-Coury [2b], Lais Mujica-Roncery [1c]

[1] Grupo de Investigación de Materiales Siderúrgicos (GMS), Ingeniería Metalúrgica, Universidad Pedagógica y Tecnológica de Colombia, Colombia. Orcid: 0000-0002-7935-4607 [a], 0000-0002-2999-5166 [b]. 0000-0003-4351-7520 [c]. Email: pablo.coha@uptc.edu.co [a], martin.mendoza@uptc.edu.co [b], lais.mujica@uptc.edu.co [c].
[2] Departamento de Materiais, Universidade Federal de São Carlos, Brasil. Orcid: 0000-0003-0792-1139 [a], 0000-0002-0457-2087 [b]. Email: gykoga@ufscar.br [a], fgcoury@ufscar.br [b].

Received: 22 June 2023. Accepted: 18 October 2023. Final version: 25 November 2023.

Abstract

A new martensitic stainless steel with high nitrogen and carbon content at low pressures was designed using the CALPHAD method. The chemical composition of the steel was checked by optical emission spectrometry, obtaining 0.17 wt%-N and 1.33 wt%-C. Scanning electron microscopy (SEM) analyses were carried out for microstructural characterization. The properties of the steel were assessed by Rockwell hardness and potentiodynamic polarization tests in 0.6M NaCl. The steel showed maximum hardness values of 60 HRC, regarded as a hard material. However, the passive film formation was prevented by the high carbon content promoting excessive Cr-rich carbides.

Keywords: martensitic; CALPHAD; high nitrogen steel, corrosion; hardness; SEM; polarization; carbide; potential; current density; tool steel; stainless steel.

Resumen

Fue diseñado mediante el método CALPHAD un nuevo acero inoxidable martensítico con alto contenido de nitrógeno y carbono a bajas presiones. La composición química del acero se verificó mediante espectrometría de emisión óptica, obteniendo 0,17% en peso de N y 1,33% en peso de C. Se realizaron análisis de microscopía electrónica de barrido (SEM) para la caracterización microestructural. Las propiedades del acero se evaluaron mediante pruebas de dureza Rockwell y polarización potenciodinámica en solución de NaCl al 0,6 M. El acero mostró valores máximos de dureza de 60 HRC, considerándose un material duro. Sin embargo, dado el alto contenido de carbono que promovió el exceso de carburos ricos en Cr, se evitó la formación de película pasiva.

Palabras clave: martensítico; acero nitrogenado; CALPHAD; corrosión; dureza; MEV; polarización; carburo; potencial; densidad de corriente; acero de herramientas; acero inoxidable.

ISSN Printed: 1657 - 4583, ISSN Online: 2145 - 8456.

How to cite: P. M. Coha-Vesga, G. Yuuki-Koga, M. E. Mendoza-Oliveros, F. Gil-Coury, L. Mujica-Roncery, "Corrosion resistance of nitrogenated high-carbon martensitic stainless steel designed and produced at nitrogen low pressures," *Rev. UIS Ing.*, vol. 22, no. 4, pp. 181-190, 2023, doi: https://doi.org/10.18273/revuin.v22n4-2023015

1. Introduction

The use of nitrogen combined in martensitic steel has demonstrated that it can improve properties like corrosion and mechanical resistance [1], making this kind of steel attractive for use in tools, bearings, ball screws, and antifriction bearing materials, among others [2]. Its applications can be seen reflected in the industrial field in sectors such as machinery manufacturing, medical equipment, and aerospace. However stainless steel can present a better corrosion resistance behavior [3].

Nitrogen, as an interstitial element shows high chemical activity and diffusion mobility even at temperatures below room temperature [4]. In conventionally produced materials, the nitrogen content is limited by the thermodynamic equilibrium that can be obtained in steel cast at atmospheric pressure, making its solubilization in steel somewhat difficult. However, higher nitrogen contents can be achieved in austenitic stainless steel at atmospheric pressure, by increasing alloying elements such as manganese and chromium [5]. Once nitrogen remains in the steel, it can promote the precipitation of nitrides, and carbides, restricting the coarsening of precipitates and matrix, improving the solid solution strengthening of the matrix as well [6], [7]. Nitrogen can replace carbon atoms, increasing some properties like corrosion resistance and hardness [8].

Nevertheless, to achieve nitrogen percentages greater than 0.1 wt%, it is recommended to use a partial pressure of nitrogen greater than 1 atm. When the N_2 pressure is between 1 and 2 atm, it is considered that sufficient nitrogen concentrations are obtained to be called nitrogenated steels [9]. The nitrogenated steels normally obtained for N_2 pressure greater than 2 atm, are considered with high nitrogen content. The problem probably is that this kind of steel is produced in special reactors with high operation pressure [10].

For this reason, over the years, the production of nitrogen steels by casting has been limited to high-pressure processes using special metallurgy, requiring expensive, complex equipment and technologies for their production [11], [12]. Processes such as pressurized electroslag remelting (PESR), pressurized plasma melting, hot isostatic compaction melting (HIP), and pressurized induction melting are commonly not available in most production plants around the world, limiting the production of this type of steel [10], [13].

To increase the solubility of nitrogen in solid solution at low pressures, it is possible to use different elements in the alloy that have an affinity for nitrogen and allow it in the solid solution [4], [9], [14]. Elements such as Ti, Cr, V, Nb, Mo, or Mn, can increase the solubility of nitrogen as long as they do not form some nitrides that could remove it from the solid solution [9].

Some authors such as Farayibi *et al.* [15] who worked with martensitic nitrogen steels, demonstrated that steels with high nitrogen content compared to nitrogen-free counterparts, showed higher microhardness values, attributed to a double effect of solid solution in the iron matrix and the formation of precipitates under different thermomechanical treatment conditions.

In a medium rich in chlorides, the corrosion potential of the material varies towards more noble zones when the nitrogen content increases. At the same time, the corrosion current density decreases. However, when the percentages of nitrogen are increased above 0.05 wt%, an inverse effect is obtained, and a decrease in the corrosion potential and pitting potential occurs, thus decreasing the corrosion resistance of the alloys [3].

Despite the benefits of nitrogen in corrosion resistance, it may happen that with the appearance of nitrides such as CrN or Cr_2N, it could impair its resistance due to pitting, and these precipitates rich in Cr can give rise to the appearance of a zone of corrosion. The Cr-depleted matrix in the vicinity of the carbides, so the passive film formed on the surface of the MSS could be weakened as well as its protective effects on the metal. In other words, these Cr-depleted zones are more susceptible to localized corrosion [3].

It has also been shown that although steel may have a chromium percentage greater than 13 wt%, the homogeneous precipitation of $M_{23}C_6$ carbides in nanometric sizes can cause a decrease in resistance to corrosion producing greater generalized chromium depletion in the material, especially for high-carbon-containing steels [16].

The relevance of this work consisted of being able to carry out the production of martensitic steel under low-pressure conditions, specifically in atmospheric conditions such as that of the city of Tunja, Colombia at 0.69 atm, taking into account that nitrogenated steels are normally produced at pressures greater than 4 atmospheres [1], [8], [17], [18], [19], [20], [21], [22], and being able to analyze some of its behavior and measurement of properties such as hardness and resistance to corrosion. Although there are studies about this kind of materials, there is still a large field of research about the behavior of this type of new materials produced under these conditions.

2. Materials and methods

2.1. Steel design and production

The design of the alloy with the elements that promote the solubility of nitrogen in the metal was calculated using the CALPHAD method, with the help of the Thermo-Calc(R) software. The database used for this design was TCFE9. The alloys were produced in an induction furnace with a controlled nitrogen atmosphere, to get equilibrium and avoid possible desorption of nitrogen to the environment upon melting and solidification, and thus avoid heterogeneous zones or the production of bubbles in the steel [1]. Si_3N_4 powder (Alfa Aesar, 85-95% purity) was used as a nitrogen source, and the pressure used in the process was the Tunja atmospheric pressure, one of the highest cities in Colombia, 2,822 m (~$7x10^4$ Pa, 0.69 atm). The diagram of the vacuum system is observed in Figure 1. Commercially available ferroalloys and cold-rolled steel were used as raw materials for the casting process.

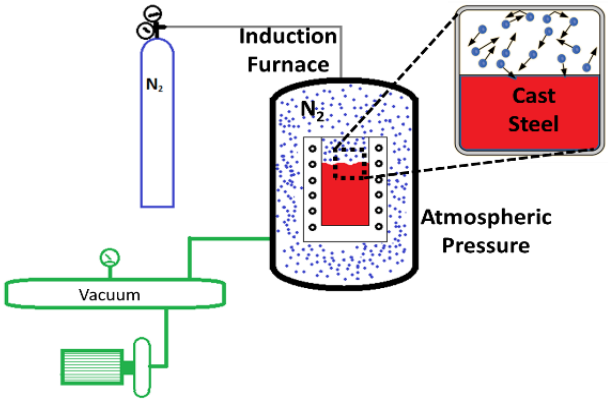

Figure 1. Diagram of vacuum induction furnace with controlled nitrogen atmosphere. Source: own elaboration.

2.2. Microstructural characterization of the material

The chemical composition of the material was measured using optical emission spectrometry, using a Q8 Magellan spectrometer, model QM/V/L. The results are presented in Table 1.

Heat treatments were carried out on the produced material, which consisted of hot deformation by forging at 1150 °C, then a spheroidization at 850 °C for 8 hours with cooling in the oven. This operation was followed by austenitization at 1030 °C for 4 hours, cooling in air and a subsequent cryogenic treatment at -196 °C for 1 hour. Finally, secondary hardening treatment by tempering was carried out at temperatures of 300, 400, 450, 500, 530, 560, and 600 °C for 2 hours with subsequent fast cooling. The analyses implemented in this research work were carried out on samples tempered from 300 to 600 °C. To name the steels, the name of the sample (1.3C) was used as a reference along with the tempering temperature, so for example, the steel tempered at 600 °C will be named in this document as 1.3C R600.

For microstructure characterization, the samples were prepared using sandpaper up to the size of 1500 grit, followed by alumina polishing and subsequently diamond paste with a particle size of 0.25 µm.

Microstructural characterization was carried out using optical microscopy (OM) and scanning electron microscopy (SEM). The MO was performed using an Olympus Microscope, model GX41, and the SEM used was Philips, model XL30 operating at 20 kV equipped with an energy-dispersive spectroscopy (EDS).

2.3. Properties Assessment

Mechanical characterization was carried out through hardness Rockwell C tests using a Rockwell Hardness Tester Beijing Time High Technology Ltd. model TH500 for all the samples. Potentiodynamic polarization curves were done on the steels using a medium rich in chlorides. A three-electrode cell set-up and a Gamry potentiostat model 600+ were used. The alloys after tempering were used as working electrodes (WE) with an exposed area of 0.3 cm^2, a saturated calomel electrode (SCE) as the reference, and a platinum grid as the counter electrode (CE). For the analysis, a standard chloride-rich solution 3.5 wt% (demineralized water and high-purity NaCl) electrolyte was used. All the analyses were done in open air at room temperature, being repeated three times for each condition to ensure repeatability. The samples were maintained at open circuit potential (OCP) for 1h, from -0.3 V against OCP up to 10^{-2} A cm^2, using 1 mV s^{-1} as the scan rate. The i_{corr} and the E_{corr} were calculated using the Tafel method since it maintain linearity within about a decade of current density relatively far from E_{corr}.

3. Results and discussion

3.1. Microstructural characterization

3.1.1. Steel design

Through Thermo-calc® the composition of the steel to be produced was designed and calculated. The affinity of elements such as chromium or manganese to maintain nitrogen within the solid solution was considered. The result of the composition that favored the solubility of

nitrogen in liquid steel was observed in Table 1. Figure 2(a) and (b) shows the pseudo-binary diagram and the phase distribution diagram for the steel.

Table 1. Chemical composition in wt% of steel produced

Sample name	Cr	Mn	Mo	Nb	C	N
1.3C	15.37	1.98	1.13	0.15	1.33	0.17

Source: own elaboration.

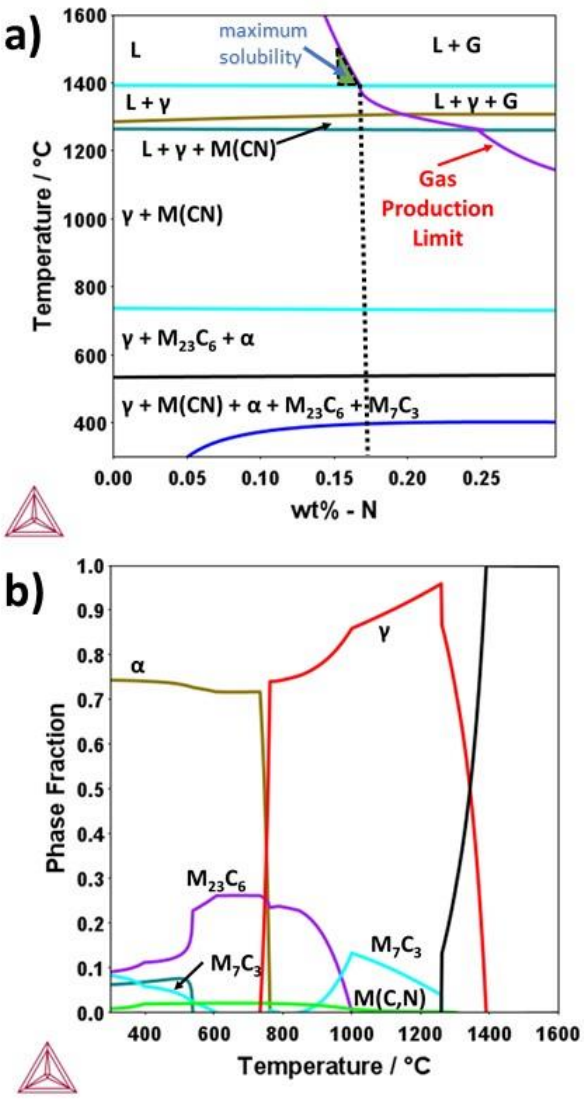

Figure 2. (a) Pseudo-binary diagram and (b) Phase fraction diagram for produced steel using the CALPHAD method. Source: own elaboration.

The thermodynamics calculation shown in Figure 2(a) indicates that in the liquid state, a percentage of around 0.18 wt%-N maximum would be obtained, before beginning the desorption of nitrogen at 1400 °C. This N content for martensitic steels is characteristic of steel with high nitrogen content, with the benefit of being achieved at low pressures of 0.69 atm. This result is relevant because, for ferritic steels, it has been found that the limit of nitrogen content is 0.08 wt% at this pressure [10]. It was also observed that in the solidification route of steel (see Figure 2(a) and (b)), some precipitates such as $M_{23}C_6$, carbonitrides and M_7C_3 are predicted. The phase that occurs in the highest volume fraction is $M_{23}C_6$, (30 vol%) at temperatures between 600 °C and 800 °C.

3.1.2. Microstructure

Figure 3 shows some micrographs of the 1.3C R400 steel produced as a reference.

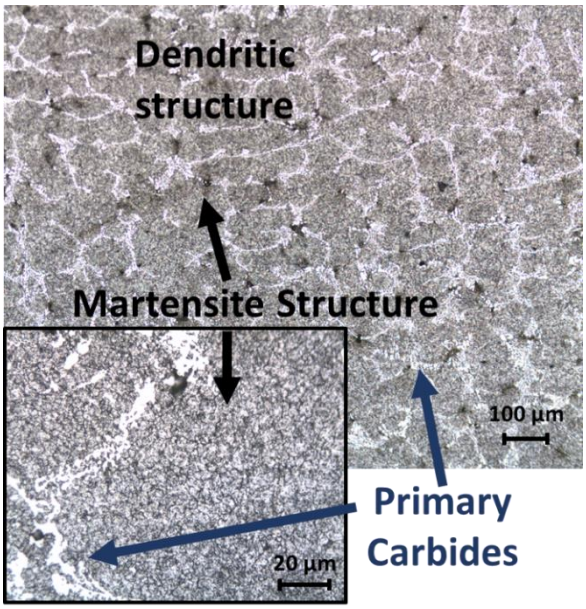

Figure 3. Optical microscopy image of sample 1.3C R400. Source: own elaboration.

The microstructure in Figure 3 shows that despite the thermal and thermomechanical treatments carried out, the sample did not achieve complete homogeneity. The solidification interface resulted in a dendritic structure. Along the dendritic arms, the formation of martensite surrounded by carbides can be observed, possibly formed in the primary solidification stage, which is observed in the thermodynamic calculations in Figure 2(b). The carbides surrounding martensite have a high-volume fraction and possibly began their formation at temperatures above 1200 °C. A priori, these carbides, due

to the amount found of them and the fact that they were not affected by the chemical etch, are related to carbides rich in chromium. Additionally, chromium is the alloying element in the highest proportion in the steels produced. This microstructure was similar in all other samples produced from this work.

Figure 4 shows images of the 1.3C R300 sample obtained with the SEM using the SE detector and the images of different elemental distribution maps.

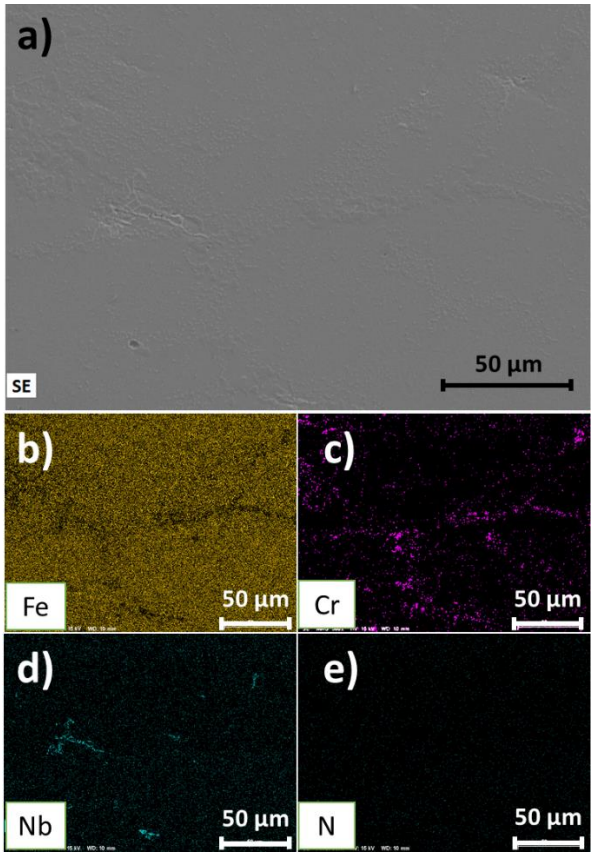

Figure 4. (a) SEM image for 1.3C R300 using SE detector. (b-e) Elemental distribution maps of Fe, Cr, Nb, and N. Source: own elaboration.

Figure 4 depicts EDS composition maps to determine the chemical distribution of the elements in the region observed in Figure 4(a). Figure 4(b) and (C) show the distribution of iron and chromium, respectively. With these two images, the formation of carbides rich in chromium was confirmed, which, as previously stated, could be inferred to correspond to primary carbides in agreement with Figure 2(b).

Carbides rich in niobium were also observed, which together with chromium carbides would increase the hardness of the material. These carbides rich in niobium are seen in Figure 4(d) and should have a stoichiometry of (Nb,Mo)C or $(Nb,Mo)(C,N)_{0,5}$ [23]. According to the thermodynamic calculations in Figure 2, these carbides are formed at temperatures around 1300 °C and are expected to be M(C,N) [1]. The presence of precipitates found in the steel can improve mechanical properties such as wear resistance or hardness, however, this can lead to an impoverishment of other properties, such as corrosion resistance [15]. Figure 4(e) shows the distribution of nitrogen in the metal matrix. Although this nitrogen measurement is qualitative due to the nature of the analysis, it indicates that the element is homogeneously distributed in the material.

Figure 5 presents the results of the cyclic polarization curves for tempered steels from 300 °C to 600 °C. Table 2 shows the results of the electrochemical parameters obtained. Although the samples have a nominal percentage of 15 wt% of chromium, they did not exhibit a high corrosion resistance. After passing the corrosion potential, the curve reveals an increase in current density, not ever displaying a passivation plateau in their electrochemical behavior. During the current density increase stage, slight oscillations were observed, possibly due to the interaction of the material trying to achieve passivation, but without any success [21], [24].

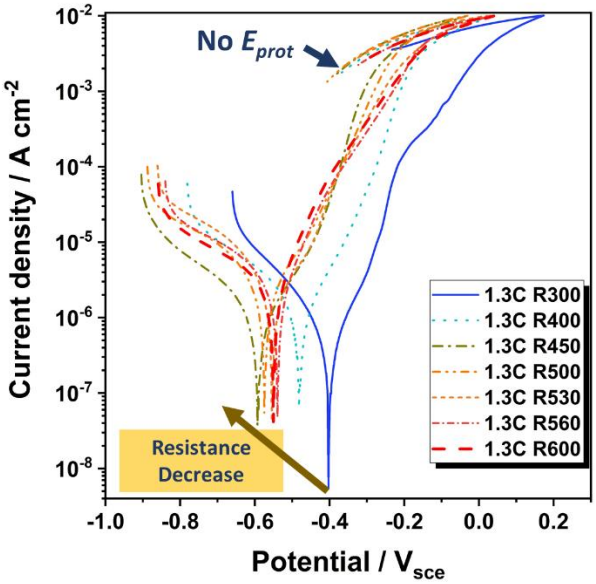

Figure 5. Cyclic potentiodynamic polarization curves for produced steels. Source: own elaboration.

As the tempering temperature increased, there was a decrease in corrosion resistance. It is observed that the sample that presented the noblest i_{corr} (1.3 ± 0.2 V) and E_{corr} (-0.41 ± 0.02 µA cm^{-2}) was the 1.3C R300. For

higher temperatures, the samples decreased their resistance, reaching a minimum E_{corr} of -0.57 ± 0.02 for the 1.3C R500 sample, and the 1.3C R530 and R560 samples seemed to improve. However, the corrosion resistance values decreased again due to part of the 1.3C R600 steel. These data are detailed in Table 2. When performing cyclic polarization, the steels did not present a passivation plateau and, therefore, no protection potential (E_{prot}).

Table 2. Electrochemical parameters resulting from cyclic polarization curves

Sample	i_{corr} / µA cm^{-2}	E_{corr} / V_{SCE}
1.3C R300	1.3 ± 0.2	-0.41 ± 0.02
1.3C R400	2.4 ± 1.2	-0.48 ± 0.01
1.3C R450	3.0 ± 0.7	-0.57 ± 0.02
1.3C R500	5.0 ± 1.0	-0.57 ± 0.02
1.3C R530	5.0 ± 1.4	-0.56 ± 0.05
1.3C R560	5.0 ± 1.1	-0.54 ± 0.03
1.3C R600	3.1 ± 1.3	-0.57 ± 0.02

Source: own elaboration.

Despite having a high chromium content, the steel did not behave like stainless steel, for example, some austenitic steels can have E_{corr} values around -0.15 V_{SCE} and i_{corr} of 0.04 µA cm^{-2} [25].

Figure 6 shows an SEM image using the secondary electron detector taken after the cyclic potentiodynamic polarization tests. The image shows the primary and secondary carbides. The primary carbides agglomerate during the solidification process of the material. These carbides are much larger and have a higher volume fraction than the secondary carbides, which, on the contrary, are distributed in the metal matrix and are of micrometric or even nanometric sizes. As seen in Figure 4(c), both types of carbides are rich in chromium. Figure 6 shows how the material was consumed by the corrosion and that the carbides were not affected due to their high chromium content. The area surrounding the carbides wears away and the carbides detach from the material. It is highlighted in Figure 6 that in the vicinity of the carbides the corrosion is more pronounced, this is due to the chromium depletion that the material suffers at the matrix-carbide interface.

Figure 7 shows a correlation between the evolution of hardness along with the increase in tempering temperature and the i_{corr} of the materials. It was observed that, as the tempering increases, a decrease in the hardness of the material takes place. This occurs because the transformation from austenite to martensite and the concentration of precipitates in the samples caused a high density of dislocations, hardening the material. As the tempering temperature increased, phenomena such as rearrangement and annihilation of dislocations, among others, occurred, relieving the internal stresses of the material.

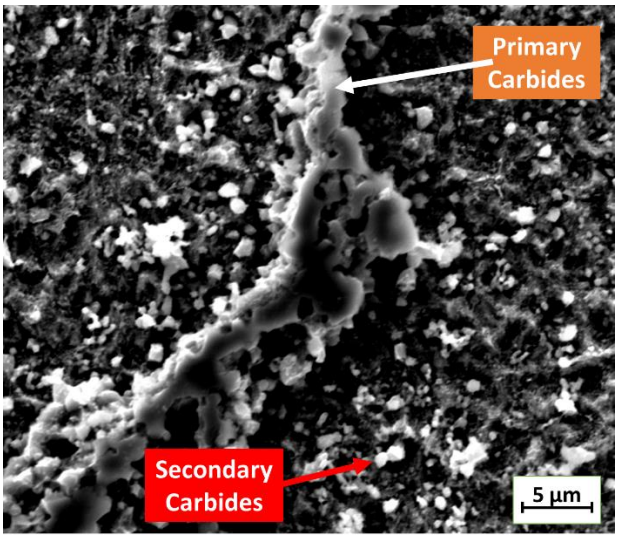

Figure 6. SEM image with SE detector. 1.3C R400 sample after the cyclic potentiodynamic polarization tests. Source: own elaboration.

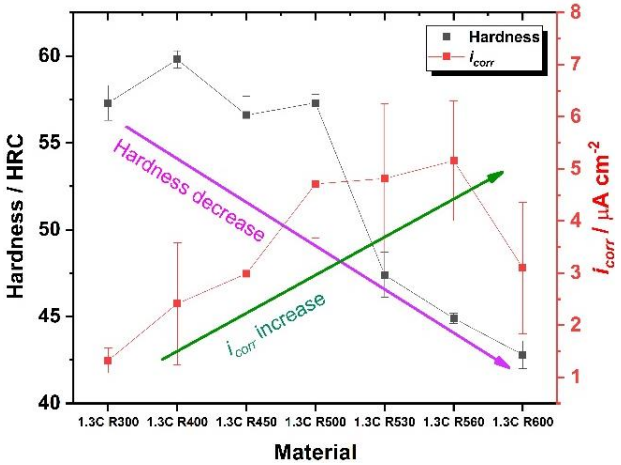

Figure 7. Comparison between hardness (HRC) and corrosion current density of steels tempered at different temperatures. Source: own elaboration.

With the hardness presented by the material, it can be inferred that the steel produced in this research work could be used as a cold work tool steel because tool steels have hardness between 50 and 60 HRC [26], [27], [28]. [29].

Likewise, an increase in the corrosion current density is observed in Figure 7, except for the 1.3C R600 sample where a slight decrease in the i_{corr} was observed. This is believed to occur because between 450 and 560 °C it is considered that the increased formation of chromium-rich carbides in the secondary hardening process, leading to matrix depletion, even though all samples have nominal 15 wt%-Cr. DLP-ER analysis coupled with diffusion calculation could be applied, but this analysis is outside the scope of the present work. At the temperature of 600 °C according to the thermodynamic calculations in Figure 2(b), a decrease in the formation of carbides occurs, especially of the M_7C_3 type, which would lead to less chromium depletion in steels.

4. Conclusion

By carrying out this research work, the following conclusions are presented:

- It was possible to design and produce a martensitic steel with high nitrogen content, at low pressures, specifically at the pressure of the city of Tunja, a city in Colombia at 2882 m height, ($7x10^4$ Pa, 0.69 atm).
- The design of the material was supported by thermodynamic calculations using the CALPHAD method and the Thermo-Calc® software, with this method the was found composition (15Cr-2Mn-1Mo-0.15Nb-1.3C) that allowed the manufacture of nitrogenated steel at low pressures were found.
- The SEM images and element distribution maps obtained allowed us to determine the presence of at least two types of precipitates (M_7C_3 and $M_{23}C_6$) in the material.
- Despite having a high chromium content (~15 wt%), the steel did not behave like stainless steel in terms of corrosion resistance with E_{corr} values like -0.57 V_{SCE} for the steel 1.3C R450, R500, and R600 and i_{corr} of 5.16 µA cm^{-2} for 1.3C R560; possibly due to the formation of chromium carbides throughout the matrix that produces a depletion of chromium content.
- As the secondary hardening temperature was increased, that is, tempering, the corrosion resistance of the material decreased, and there was no noticeable recovery; possibly because the temperature influenced the production of carbides which led to a depletion of chromium in the matrix.
- The material presented high hardness values, especially the sample 1.3C R400 with a hardness close to 60 HRC that could allow it to be developed as a cold work tool steel because this type of steel has a hardness similar to this value.
- Although this steel has the potential to have applications as a cold work tool steel due to its high hardness values, it could not be used as a stainless steel due to its low corrosion resistance.

Based on this work, the authors recommend carrying out studies on the mechanisms of chromium depletion in the material matrix. It is also recommended to continue the search for elements in the appropriate proportions that allow for achieving higher nitrogen solubilities in a ferritic matrix.

Acknowledgments

The authors thank everyone who in one way or another helped to carry out this research work. We thank the staff of the Pedagogical and Technological University of Colombia (UPTC), as well as the professors, technicians, and other personnel of the Federal University of Sao Carlos (UFSCar) for all the support provided. The authors thank the Laboratory of Structural Characterization (LCE/DEMa/UFSCar) for the general facilities.

Funding

Pablo Coha especially thanks the Ministry of Science, Technology and Innovation (Minciencias) of Colombia for the financial support received with the “Becas de Excelencia Doctoral del Bicentenario” program. Guilherme Yuuki Koga gratefully acknowledges the financial support of CNPq Universal Grant No. 407651/2021-7

Autor Contributions

P. M. Coha-Vesga: Investigation, Conceptualization, Methodology, Formal analysis, Writing Original Draft & Editing. M. E. Mendoza-Oliveros: Methodology, Analysis, Review & Editing. L. Mujica-Roncery: Supervision, Review & Editing, Project administration.

All authors have read and agree to the published version of manuscript.

Conflicts of Interest

The authors declare no conflict of interest.

Institutional Review Board Statement

Not applicable.

Informed Consent Statement

Not applicable.

References

[1] P. M. Coha-Vesga, M. E. Mendoza-Oliveros, F. R. Pérez-Villamil, F. Coury, and L. Mujica-Roncery, "Novel Martensitic High Carbon-Nitrogen Steel Produced by Casting at Low Pressure," *steel Res. Int.*, Oct. 2022, doi: https://doi.org/10.1002/srin.202200686

[2] N. B. Dhokey, A. Upadhye, N. Shah, and K. T. Tharian, "Transition in wear behavior and mechanical properties of novel high nitrogen martensitic steel in cryogenic temperature regimes," *Mater. Today Proc.*, vol. 43, pp. 3023–3029, 2021, doi: https://doi.org/10.1016/j.matpr.2021.01.367

[3] X. Qi, H. Mao, and Y. Yang, "Corrosion behavior of nitrogen alloyed martensitic stainless steel in chloride containing solutions," *Corros. Sci.*, vol. 120, pp. 90–98, May 2017, doi: https://doi.org/10.1016/j.corsci.2017.02.027

[4] V. G. Gavriljuk and H. Berns, *High Nitrogen Steels*. Berlin, Heidelberg: Springer Berlin Heidelberg, 1999. doi: https://doi.org/10.1007/978-3-662-03760-7

[5] G. O. Rhodes and J. J. Conway, "High-nitrogen austenitic stainless steels with high strength and corrosion resistance," *JOM*, vol. 48, no. 4, pp. 28–31, Apr. 1996, doi: https://doi.org/10.1007/BF03222915

[6] N. Shah, K. Arora, N. B. Dhokey, N. Dileep Kumar, and K. T. Tharian, "Studies on Wear Behaviour and DBTT in Sub-zero Regimes of Cryo-Treated High Nitrogen Martensitic Stainless Steel (HNMS)," *Trans. Indian Inst. Met.*, vol. 72, no. 8, pp. 2121–2126, Aug. 2019, doi: https://doi.org/10.1007/S12666-018-01555-2

[7] A. Bénéteau, P. Weisbecker, G. Geandier, E. Aeby-Gautier, and B. Appolaire, "Austenitization and precipitate dissolution in high nitrogen steels: an in situ high temperature X-ray synchrotron diffraction analysis using the Rietveld method," *Mater. Sci. Eng. A*, vol. 393, no. 1–2, pp. 63–70, Feb. 2005, doi: https://doi.org/10.1016/J.MSEA.2004.09.054

[8] D. H. Ping and M. Ohnuma, "ω-Fe particle size and distribution in high-nitrogen martensitic steels," *J. Mater. Sci.*, vol. 53, no. 7, pp. 5339–5355, Apr. 2018, doi: https://doi.org/10.1007/s10853-017-1938-0

[9] G. Stein and I. Hucklenbroich, "Manufacturing and Applications of High Nitrogen Steels," *Mater. Manuf. Process.*, vol. 19, no. 1, pp. 7–17, Dec. 2004, doi: https://doi.org/10.1081/AMP-120027494

[10] H. B. Li, Z. H. Jiang, Q. F. Ma, and D. P. Zhan, "Some Theoretical Problems Analysis of Melting High Nitrogen Stainless Steels," *Adv. Mater. Res.*, vol. 455–456, pp. 103–109, Jan. 2012, doi: https://doi.org/10.4028/www.scientific.net/AMR.455-456.103

[11] A. G. Svyazhin, S. P. Efimenko, and L. M. Kaputkina, "The Problems of High-Nitrogen Steels Production," *Mater. Sci. Forum*, vol. 318–320, pp. 353–358, Oct. 1999, doi: https://doi.org/10.4028/www.scientific.net/MSF.318-320.353

[12] L. Zhekova and T. Rashev, "Feasibility study on developing high-nitrogen steels by refining in suspended state under high pressure," *Metallurgist*, vol. 51, no. 1–2, pp. 90–96, Jan. 2007, doi: https://doi.org/10.1007/s11015-007-0018-0

[13] H. Feng *et al.*, "Influence of nitrogen on corrosion behaviour of high nitrogen martensitic stainless steels manufactured by pressurized metallurgy," *Corros. Sci.*, vol. 144, pp. 288–300, Nov. 2018, doi: https://doi.org/10.1016/j.corsci.2018.09.002

[14] H. Berns, V. G. (Valentin G. Gavriliuk, and S. Riedner, *High interstitial stainless austenitic steels*. Springer, 2013.

[15] P. K. Farayibi, M. Blüm, and S. Weber, "Densification of a high chromium cold work tool steel powder in different atmospheres by SLPS: Microstructure, heat treatment and micromechanical properties," *Mater. Sci. Eng. A*, vol. 777, p. 139053, Mar. 2020, doi: https://doi.org/10.1016/j.msea.2020.139053

[16] S.-Y. Lu, K.-F. Yao, Y.-B. Chen, M.-H. Wang, and X.-Y. Ge, "Influence of Heat Treatment on the Microstructure and Corrosion Resistance of 13 Wt Pct Cr-Type Martensitic Stainless Steel," *Metall. Mater. Trans. A*, vol. 46, no. 12, pp. 6090–6102, Dec. 2015, doi: https://doi.org/10.1007/s11661-015-3180-1

[17] H. Feng *et al.*, "Significance of Partial Substitution of Carbon by Nitrogen on Strengthening and Toughening Mechanisms of High Nitrogen Fe-15Cr-1Mo-C-N Martensitic Stainless Steels," *Metall. Mater. Trans. A*, vol. 50, no. 11, pp. 4987–4999, Nov. 2019.

[18] H. Berns, N. Krasokha, and M. Seifert, "Nitrogen and Ausforming to Improve Stainless Martensitic Steels," *steel Res. Int.*, vol. 85, no. 7, pp. 1200–1208, Jul. 2014, doi: https://doi.org/10.1002/srin.201300299

[19] O. A. Bannykh, V. M. Blinov, and M. V. Kostina, "Structure and Properties of Low-Alloy High-Nitrogen Martensitic Steels," *Met. Sci. Heat Treat. 2003 451*, vol. 45, no. 1, pp. 43–48, 2003, doi: https://doi.org/10.1023/A:1023952230778

[20] A. V. Elistratov, V. M. Blinov, A. G. Rakhshtadt, A. A. Aliev, A. N. Malofeeva, and A. D. Davydov, "Effect of the Chemical Composition and Structure of High-Chromium-Nitrogen Steels on Their Corrosion Resistance," *Met. Sci. Heat Treat.*, vol. 45, no. 9/10, pp. 385–389, Sep. 2003, doi: https://doi.org/10.1023/B:MSAT.0000009786.65463.78

[21] H. Feng *et al.*, "Designing for high corrosion-resistant high nitrogen martensitic stainless steel based on DFT calculation and pressurized metallurgy method," *Corros. Sci.*, vol. 158, p. 108081, Sep. 2019, doi: https://doi.org/10.1016/j.corsci.2019.07.007

[22] X. Cai, X.-Q. Hu, L.-G. Zheng, and D.-Z. Li, "Hot Deformation Behavior and Processing Maps of 0.3C–15Cr–1Mo–0.5N High Nitrogen Martensitic Stainless Steel," *Acta Metall. Sin. (English Lett.*, vol. 33, no. 5, pp. 693–704, May 2020, doi: https://doi.org/10.1007/s40195-019-00991-3

[23] J. Speer, C. M. Enloe, K. Findley, C. Vantyne, and E. Pavlina, "Solubility and Precipitation of Carbides Containing Niobium and Molybdenum in Low Alloy Steels," Apr. 2015.

[24] G. T. Burstein, "Understanding Localized Corrosion through Electrochemical Measurements," *ECS Trans.*, vol. 3, no. 31, pp. 193–204, Sep. 2007, doi: https://doi.org/10.1149/1.2789227

[25] J. Ramírez *et al.*, "Effect of solution annealing temperature on the localised corrosion behaviour of a modified super austenitic steel produced in an open-air atmosphere," *Mater. Chem. Phys.*, vol. 299, p. 127498, Apr. 2023, doi: https://doi.org/10.1016/j.matchemphys.2023.127498

[26] C. E. Pinedo, *Tratamentos Térmicos e Superficiais dos Acos*, 1st ed. Sao Paulo: Edgard Blucher Ltda., 2021.

[27] R. Rejeesh *et al.*, "Relative effect of B and N concentrations on the microstructural stability and mechanical properties of modified 9Cr-1Mo steel," *J. Alloys Compd.*, vol. 867, p. 158971, Jun. 2021, doi: https://doi.org/10.1016/j.jallcom.2021.158971

[28] L. Bourithis, G. D. Papadimitriou, and J. Sideris, "Comparison of wear properties of tool steels AISI D2 and O1 with the same hardness," *Tribol. Int.*, vol. 39, no. 6, pp. 479–489, Jun. 2006, doi: https://doi.org/10.1016/j.triboint.2005.03.005

[29] J. Ravagli-Reyes, E. Pérez-Ruiz, and J. Llano-Martínez, "Estudio del grado de endurecimiento y resistencia al desgaste por deslizamiento del acero AISI 1045 endurecido por temple con refrigerante automotory para mecanizado," *Rev. UIS Ing.*, vol. 18, no. 2, pp. 113–118, Feb. 2019, doi: https://doi.org/10.18273/revuin.v18n2-2019010